



Reaching trajectories unravel modality-dependent temporal dynamics of the automatic process in the Simon task: a model-based approach

Yael Salzer^{1,2} · Jason Friedman^{3,4} 

Received: 26 September 2018 / Accepted: 28 March 2019
© Springer-Verlag GmbH Germany, part of Springer Nature 2019

Abstract

The Simon effect represents a phenomenon in which the location of the stimuli affects the speed and accuracy of the response, despite being irrelevant for the task demands. This is believed to be due to an automatic activation of a response corresponding to the location of the stimuli, which conflicts with the controlled decision process based on relevant stimuli features. Previously, differences in the nature of the Simon effect (i.e., the pattern of change of the effect across the distribution of response times) between visual and somatosensory stimuli were reported. We hypothesize that the temporal dynamics of visual and somatosensory automatic and controlled processes vary, thus driving the reported behavioral differences. While most studies have used response times to study the underlying mechanisms involved, in this study we had participants reach out to touch the targets and recorded their arm movements using a motion capture system. Importantly, the participants started their movements before a final decision was made. In this way, we could analyze the movements to gain insights into the competition between the automatic and controlled processes. We used this technique to describe the results in terms of a model assuming automatic activation due to location-based evidence, followed by inhibition. We found that for the somatosensory Simon effect, the decay of the automatic process is significantly slower than for the visual Simon effect, suggesting quantitative differences in this automatic process between the visual and somatosensory modalities.

Introduction

The spatial location of target stimuli, despite being task irrelevant, has consistently been shown to have an effect on performance (Simon, & Wolf, 1963). In a typical Simon task, the task may be to press the left or right button depending on the color of the stimuli. While the location of the stimuli has no bearing on the correct response (left or right), participants are less accurate and take longer to select which button to press when the location of the stimulus is incongruent with the correct response relative to when they are congruent (i.e., Simon

effect). It is assumed that this response selection conflict is due to some form of involuntary processing or activation of the spatial information (Simon, 1990). The temporal dynamics of the response selection conflict are typically studied by examination of the pattern of change of the Simon effect across the distribution of response times (RTs) (De Jong, Liang, & Lauber, 1994; Proctor, Miles, & Baroni, 2011). The distribution of RTs for congruent and incongruent trials is partitioned into quantiles and the Simon effect is calculated for each quantile separately (De Jong et al., 1994; Ratcliff, 1979; Ridderinkhof, 2002). The dynamics of the Simon effect across the distribution are visualized by plotting the relative effect for each quantile as a function of the mean RT quantile across conditions (i.e., delta plots). Depending on the modality of the stimulus, and details of the experiment, various delta plot patterns have been recorded. In some, the Simon effect increased, in others it decreased, or did not change as function of the mean response time (Salzer, Aisenberg, Oron-Gilad, & Henik, 2014; Töbel, Hübner, & Stürmer, 2014; Xiong, & Proctor, 2016). This variety in patterns is noteworthy, because it is the root of several disputes (for a review see Salzer et al., 2017). First, are the increasing and decreasing slopes the outcome of a common or two separate mechanisms? Wascher

✉ Jason Friedman
jason@tau.ac.il

¹ Department of Psychology, Ben-Gurion University of the Negev, Beersheba, Israel

² Institute of Agricultural Engineering Agricultural Research Organization (A.R.O) - Volcani Center, Derech-Hmakabim 68, 7528809 Rishon-Le'Zion, Israel

³ Department of Physical Therapy, Sackler Faculty of Medicine, Tel Aviv University, POB 39040, 6997801 Tel Aviv, Israel

⁴ Sagol School of Neuroscience, Tel Aviv University, Tel Aviv, Israel

et al. (2001) and Wiegand and Wascher (2005, 2007) have argued that increasing (e.g., somatosensory) and decreasing (i.e., horizontal visual) Simon effects are the result of two different processes: ‘visuomotor Simon effect’ and a ‘cognitive Simon effect’. This view was contradicted in a recent review (Salzer, de Hollander, & Forstmann, 2017) where the authors have argued in favor of a general common interference mechanism over the account of two separate mechanisms, as is suggested by findings of both increasing and decreasing slopes, regardless of the modality. The visual modality dominates the literature on cognitive control and conflict resolution, and it is generally agreed that the components of the stimulus–response conflict, as in the Simon task, are driven from modality-specific neural pathways (Salzer et al., 2017). Thus, it might be that conclusions drawn from a visual Simon task are relevant only to the visual modality. To make conclusions more generally related to conflict resolution, a comparison between modalities is needed. Second, is a decrease in the delta plots the outcome of active inhibition or passive decay of the irrelevant process? To complicate the situation, many mathematical models of perceptual decision making, such as the prominent drift diffusion model (Ratcliff, & McKoon, 2008), are unable in their basic form to fit to the data from the Simon task (Schwarz, & Miller, 2012).

Diffusion model for conflict

A recently proposed diffusion model for conflict (DMC, Ulrich, Schröter, Leuthold, & Birngruber, 2015) succeeded where others have failed; it can account for data from a wide range of conflict tasks. The model captures two parallel processes, direct response (automatic) activation of the task-irrelevant spatial location of the stimulus and deliberate indirect (controlled) processing of task-relevant feature (De Jong et al., 1994). In the DMC, a standard drift diffusion model, with a constant drift rate, represents the deliberate process. The additional process that represents the direct response is modeled as a gamma distribution. It increases to a maximum and then decays. The model does not aim to determine what mechanism underlies the gamma function, whether it is active inhibition of the irrelevant process (Ridderinkhof, 2002) or merely spontaneous decay (Hommel, 1994). These two processes are summed by a single accumulator. When the summed activation of the two processes reaches a predetermined bound, as with the standard drift diffusion model, a decision is made. By changing the shape of the gamma distribution, it becomes possible to capture the different delta plots observed (positive, neutral or negative). It is noteworthy that the parameters associated with the standard drift diffusion show strong recovery, whereas the parameters for the gamma distribution are not well recovered (White, Servant, & Logan, 2018).

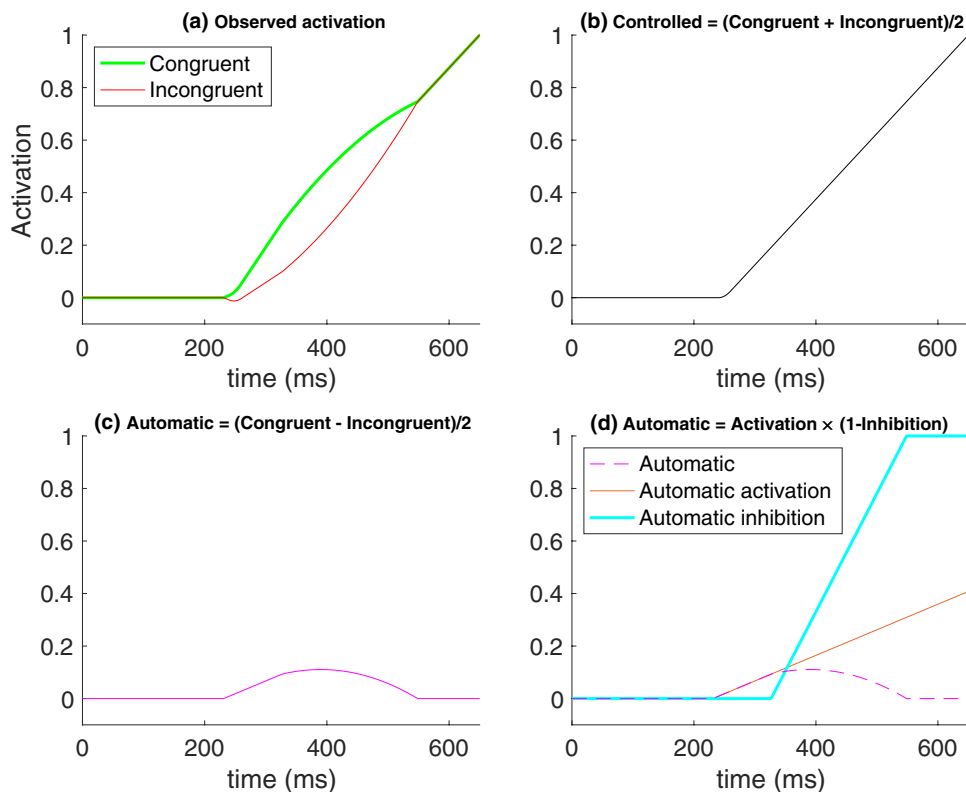
Continuous arm movements

Whilst sequential sampling models suggest a way of modeling the temporal dynamics of the underlying process, the predictions are made regarding the end of the process, namely the response time (i.e., response termination). However, the conflict resolution is assumed to take place at an earlier time, before the response was executed (Ulrich et al., 2015). We refer to the decision made at the response time in a typical two-alternative forced choice task as the final decision. Several studies have used reach-to-target movements in place of button press responses to observe the state of the decision process before this final decision is made. Using a continuous response, it is possible to access the state of the decision-making process (which is also assumed to be continuous) before the final decision is made (Finkbeiner, Coltheart, & Coltheart, 2014; Friedman, Brown, & Finkbeiner, 2013; Spivey, Grosjean, & Knoblich, 2005). These methods are based on observing proxies for the current status of the decision process, which is still undergoing and hence has not yet reached one of the two options, at times before the final decision is made. For the Simon effect, arm movement studies have shown that when the trajectories of the fingertip are recorded during the response selection (i.e., before the final decision is made), participants’ movements are initially biased towards the imperative stimuli location, i.e., the location of the stimuli rather than the correct response (Buetti, & Kerzel, 2009; Finkbeiner, & Heathcote, 2016; Welsh, Pacione, Neyedli, Ray, & Ou, 2015). The activation towards the stimuli can be observed as partial errors, which are small electromyography (EMG) bursts in a response-related muscle on the side of the stimuli location (Servant, White, Montagnini, & Burle, 2016). When response selection and movement execution are artificially separated by the experimental protocol, the Simon effect can be observed in both phases of the response (Scorolli, Pellicano, Nicoletti, Rubichi, & Castiello, 2014). Further, it was found that the Simon effect is better described by an account where the automatic activation (based on stimuli location) starts earlier than the controlled process (based on the relevant information), compared to an account based on magnitude differences in terms of the automatic and controlled processes (Finkbeiner, & Heathcote, 2016).

Activation–inhibition (AI) model

In this paper, we present and apply a model we termed the activation–inhibition model, based on the model proposed in Ridderinkhof (2002). As our goal is to model the decision-making process as it is taking place, rather than the end of the process (which is typically the response time), we model the amount of activation (i.e., evidence

Fig. 1 Schema of decomposition of the activation. **a** An example of observed activation in an experiment. The observed activation is assumed to be the sum of the controlled and automatic processes, with the automatic process assumed to have equal magnitude but positive sign for congruent trials, and negative sign for incongruent trials. Based on this, we can calculate **b** the controlled process as half the sum of the congruent and incongruent activations. Similarly, we can calculate **c** the automatic process as half the difference between congruent and incongruent activations. The automatic process can then be decomposed into an automatic activation, and delayed inhibition. When the inhibition reaches 1, the automatic component no longer has an effect



accumulation) as a function of time. Similar to the DMC model, we assume that there is a deliberate, controlled process based on the content of the stimuli, which gradually increases its activation as a function of time. Additionally, we assume that there is an automatic process that is driven by the stimuli location, which similarly increases its activation as a function of time. The location-based activation is gradually inhibited by a separate process until it no longer has an effect. We assume that we can observe the sum of these activations as a function of time from the kinematic data, described in detail below. When the activation reaches a bound, then the final decision has been made.

Based on this model, we assume that the observed overall activation (see Fig. 1a) is the sum of the automatic and controlled responses. We assume that the automatic response is equal in magnitude in the congruent and incongruent cases (only in opposite directions). If we sum the congruent and incongruent activations, we are left with two times the controlled process (as the congruent and incongruent automatic activations cancel out). Hence, taking half the sum of the congruent and incongruent responses provides the controlled process (see Fig. 1b). Similarly, if we subtract the incongruent activation from congruent activation, then the controlled process cancels out, and we are left with two times the automatic response. Thus, taking half of the difference between the activation in the incongruent response from the activation in the congruent response leaves us with the automatic

response (see Fig. 1c). If we assume that the automatic activation and the selective inhibition are also linear processes, we can also find the onset time and slopes of these processes (see Fig. 1d).

In this study, we accessed the current amount of information accumulated (i.e., activation) using proxy, cumulative submovement amplitudes (Finkbeiner, & Friedman, 2011), described in more detail below. This technique is a way of observing the state of the decision-making process at time points before the final decision is made. We will use this technique to test whether the proposed activation–inhibition model can be fit to the data.

The relative processing speed of the spatial and non-spatial attributes of the stimulus is dependent on modality-specific neural pathways, modulated by the nature and complexity of the stimulus, and reflected in delta plot slopes (Salzer et al., 2017). In particular, while with horizontally aligned visual stimuli the Simon effect decays, with horizontal somatosensory stimuli the Simon effect does not decay (Salzer et al., 2014; Töbel et al., 2014). The difference in delta plots between the visual and somatosensory versions of task may serve to our benefit as an amplifier of the phenomena. We predict that the activation–inhibition model will be able to be fit to data for both tasks. The model may fail for one of the modalities if, for example, there is automatic activation but no subsequent inhibition.

We hypothesize that both the onset of the activation and the inhibition of the automatic process for visual stimuli will take place significantly earlier than for the somatosensory stimuli, based on faster responses observed in previous studies for visual stimuli (Salzer, 2013; Salzer et al., 2014). As the targets are quite distinct in both modalities, we assume that the rate of uptake will be similar for the visual and somatosensory stimuli. The goal of this study is to determine whether the previously observed differences in the Simon affect for different modalities and setups can be explained by timing and gain differences in terms of the inhibition processes, i.e., can a single process model successfully model the Simon effect in its different forms?

Methods

Participants

Sixteen undergraduate students (ten females; 22–33 years of age, mean = 25 years) from Tel Aviv University took part in the experiment. Participants were reimbursed for participation in the experiments (60 shekels in total). Informed consent was obtained from all individual participants included in the study. The participants signed an informed consent form before starting the experiment, and the experiment was approved by the Tel Aviv University Human Ethics committee.

Apparatus

The responses were recorded using a Polhemus Liberty magnetic motion capture system, recording at 240 Hz, with the sensor taped to the fingernail of the index finger on the right hand. Each trial started at the same position, marked by a sticker (5 cm from the edge of the table), and the responses involved reaching out and touching a sticker on one of the two wooden targets placed next to the monitor (see Fig. 2). Participants were instructed to touch the wooden targets instead of the screen due to limitations of the magnetic motion capture system. A similar setup, with its lack of spatial overlap between the stimulus and target has been used previously for studying the Simon effect (Finkbeiner, & Heathcote, 2016), where strong Simon effects were observed. Each target was 43 cm horizontally (left or right) from the starting position, 34 cm in front of the starting position and at a height of 25 cm. The location of the sensor on the fingernail while the participants touched the start point and the two targets were recorded immediately prior to the experiment, and were used in



Fig. 2 Experimental setup. The participants started each trial with their hand on the green sticker near the edge of the table. They were instructed to reach out and touch the relevant target (sticker on the poles on the left or right), based on the stimulus (visual or somatosensory), and to start moving on the third beep. The trial ended when the participant touched one of the two targets. The x , y and z axis are shown, and the analysis of the movement data was performed in 2D (x - y plane)

the experiment to identify when the subject was at the start position or at one of the targets. The instructions and visual stimuli were shown on a 24" monitor (Samsung S24B300, 52.2 cm \times 29.6 cm, 1920 \times 1080 pixels). Participants wore circumaural headphones during all experiments, to block external noise and play white noise to prevent hearing the somatosensory stimulation, and to deliver beeps which were used to indicate the start of a trial and provide feedback. The experiment was run using the Repeated Measures software (Friedman, 2014), Matlab software which runs on top of the Psychophysics toolbox (Brainard, 1997).

Visual target

The visual target stimulus was a white outline of a triangle or a square against the black screen background. An equal number of triangle and square stimuli were introduced. The figures appeared on either the right or left side of the screen (see Fig. 2). For half of the participants, the correct response to triangle stimuli was to reach out and touch the left touch base with their index finger, and the correct response to the continuous stimuli was to reach out and touch the right touch base with the right index finger. For the other half of the participants, the mapping was the opposite. In the congruent condition, both the target and correct response were on the same side. In the incongruent condition, they were contralateral.

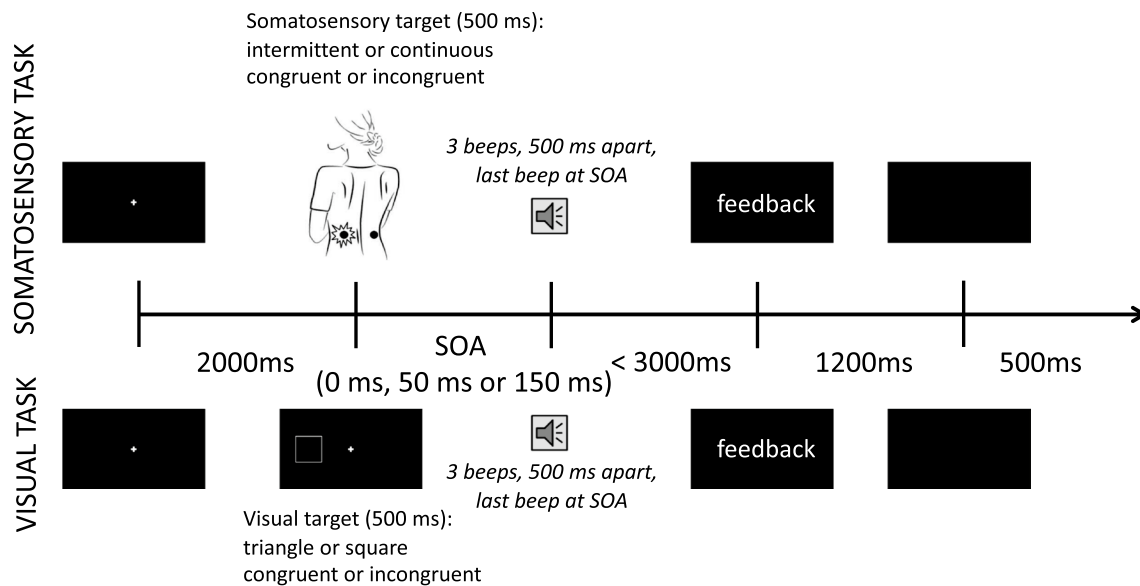


Fig. 3 Experimental procedure. After a fixation point was shown for 2000 ms, the target was presented for 500 ms (somatosensory or visual). SOA was at either 0 ms, 50 ms, or 150 ms. Three beeps were produced 500 ms apart, with the last beep at SOA indicating the go

signal. Participants were required to start moving between 100 ms before to 300 ms after the go signal. Following the arm movement, visual feedback was provided when the response was incorrect or no response was made

Vibrotactile system

Two C2 tactors (i.e., vibrating somatosensory actuators), powered by an Eval 2.0 controller (Engineering Acoustics Inc.), were stitched to an elastic-fiber strap. The strap was worn around the torso at the waist level over the participant's clothing. The distance between the left and right vibrotactors was 27 cm. The elastic-fiber strap stretched to fit different waistlines, therefore it should be noted that these distances were not firmly fixed between participants. One vibrotactor was positioned to the left of the spinal column (left vibrotactor), and the other to the right of the spinal column (right vibrotactor), as shown in Fig. 3.

Somatosensory target

The somatosensory target stimulus was the same as used previously (Salzer et al., 2014): a 250 Hz vibration of either a single continuous 500 ms pulse (i.e., continuous stimulus) or a fast sequence of five equally spaced 50 ms pulses with a total duration of 500 ms (i.e., intermittent stimulus). An equal number of intermittent and continuous stimuli were introduced in both the practice and experimental blocks, activated by either right or left tactors. For half of the participants, the correct response to the continuous stimuli was moving the hand to touch the left touch base, and the correct response to the continuous stimuli was moving the hand to touch the right touch base. For the other half of the participants, the mapping was the opposite. In the

congruent condition, both the target and correct response were on the same side. In the incongruent condition, they were contralateral.

Design

Half of the participants were assigned to the somatosensory task first and the other half to the visual task first. Each session included 480 trials, taking approximately 1 h. The two sessions ran on separate days.

Experimental procedure

The participant sat in front of a table. For the somatosensory task, at the beginning of the experiment, the experimenter verified that both tactors were equally sensed and comfortably placed on the participant's back. Each participant was introduced and familiarized with the sensation of intermittent and continuous stimuli for both tactors. Headphones delivering white noise and the beeps were worn in both somatosensory and visual conditions.

Each trial began with a fixation cross displayed for 2000 ms at the center of the computer screen (see Fig. 3). After this, the target was activated (or displayed), for 500 ms. Three stimulus-onset asynchronies (SOA, i.e., the time between stimulus onset and the go signal) were used: 0 ms, 150 ms and 250 ms (as used in Finkbeiner et al., 2014), with equal probabilities, to sample the decision process of the participants at a broad range of times. The go

signal was the third of three beeps, with a gap of 500 ms between the beeps. The participant was required to start moving within a response window, 100 ms before the go signal to 300 ms after the go signal. Visual and audio feedbacks were provided if the participant generated a response outside this window (“Too early!” or “Too late!” shown on the screen, combined with a buzzing sound). The fixation cross remained on the screen until a response was produced or 3000 ms passed. For an incorrect response (reaching to the wrong target), the feedback message “Incorrect answer” was displayed for 1200 ms; if no response was collected, the message “No response received” was displayed; otherwise, the screen remained blank. Following this, the screen was blank for another 500 ms before a new trial began.

Analysis

The position data were filtered using a two-way low-pass fourth-order Butterworth filter, with a cutoff of 20 Hz. The constraints of the experiment required participants to start moving at different times, providing us with movements that began at different times post-stimulus onset. Due to the large amount of variation between individual trajectories, we fitted orthogonal polynomials, using a variant of the orthogonal polynomial trend analysis (OPTA) procedure (Finkbeiner et al., 2014; Finkbeiner, & Heathcote, 2016; Karayanidis, Provost, Brown, Paton, & Heathcote, 2011; Woestenburg, Verbaten, van Hees, & Slangen, 1983). Specifically, we ordered the trajectories of the correct trials for a single experiment cell (participant, congruent/incongruent, left/right, somatosensory/visual) by movement initiation time (MIT), then fit all the x (left–right) velocities for a single participant, using only the order of the trial as the covariate, using 12th order orthogonal polynomials (after subtracting the mean velocity). This procedure thus quantified the changes in the velocities as a function of MIT as linear changes in the amplitudes of the 12th order orthogonal polynomials. We then binned the MITs into 20 bins and computed the velocity profiles for each bin for each participant. This method is preferable to simply averaging the velocities due to the enormous variation between repetitions of such a test—the OPTA procedure has been shown to significantly reduce the signal-to-noise ratio (Woestenburg et al., 1983).

The remainder of our analysis relies on the widely held assumption that our movements are composed of discrete, overlapping submovements (Flash, & Henis, 1991; Friedman et al., 2013). By assumption, each submovement is discrete and ballistic, that is, its amplitude, direction and duration are all planned before the movement onset. This feature allows us to probe the current movement intent at the time of submovement onset. By pooling data from many repetitions, we can observe how the movement goal changes as a function of time (Finkbeiner, & Friedman, 2011).

To perform this analysis, we decomposed the movements into submovements, by finding the best set of submovements that approximate the observed movement. The decomposition was performed in 2D (in the horizontal x – y plane), as these are the primary directions of interest. Each submovement is modeled according to the minimum jerk criterion (Flash, & Hogan, 1985), i.e., its velocity profile is given by (1):

$$\dot{x}(t) = D_x \left(30 \left(\frac{t - T_0}{D} \right)^4 - 60 \left(\frac{t - T_0}{D} \right)^3 + 10 \left(\frac{t - T_0}{D} \right)^2 \right), \quad (1)$$

where D_x is the amplitude of the movement, T_0 is the movement onset time, D is the duration of the movement, and t is time which goes from $T_0 \leq t \leq T_0 + D$. Each minimum jerk submovement has a bell-shaped velocity profile. We used minimum jerk submovements rather than some other form of submovement, because they are commonly used for decomposition, and there is not another form that provides a better fit with equal or fewer parameters (Horowitz, Majeed, & Patton, 2016). The reconstructed velocity profile $F(t)$ is then given by the superposition (summation) of one or more submovements (2):

$$F(t) = \sum_{i=1}^N \begin{cases} 0 & t < T_{0i} \\ \dot{x}_i(t) & T_{0i} \leq t \leq T_{0i} + D_i \\ 0 & t > T_{0i} + D_i \end{cases}, \quad (2)$$

where the values subscripted with an i correspond to the i th submovement. While the above equations are for movement in the x direction, equivalent expressions can be written for movement in the y direction. A reconstruction cost is defined by (3) (Friedman, & Finkbeiner, 2010):

$$E = \sum_r \frac{(F_x(t) - G_x(t))^2 + (F_y(t) - G_y(t))^2 + (F_v(t) - \sqrt{G_x(t)^2 + G_y(t)^2})^2}{2(G_x(t)^2 + G_y(t)^2)}, \quad (3)$$

where $G_x(t)$ and $G_y(t)$ are the observed x and y components of the hand velocity, and $F_x(t)$ and $F_y(t)$ are the reconstructions of the x and y components. $F_v(t)$ is the reconstructed tangential velocity, it is included to prevent the optimization procedure from selecting two approximately simultaneous submovements with large but opposite velocities. The optimization technique then minimizes this error, which was implemented using the constrained nonlinear optimization function in Matlab. The initial parameter values were randomly selected, and the procedure was run ten times, for 1–4 submovements (Rohrer, & Hogan, 2006). The least number of submovements with reconstruction error of less than 0.03 was selected. An example of submovement decomposition is shown in Fig. 4.

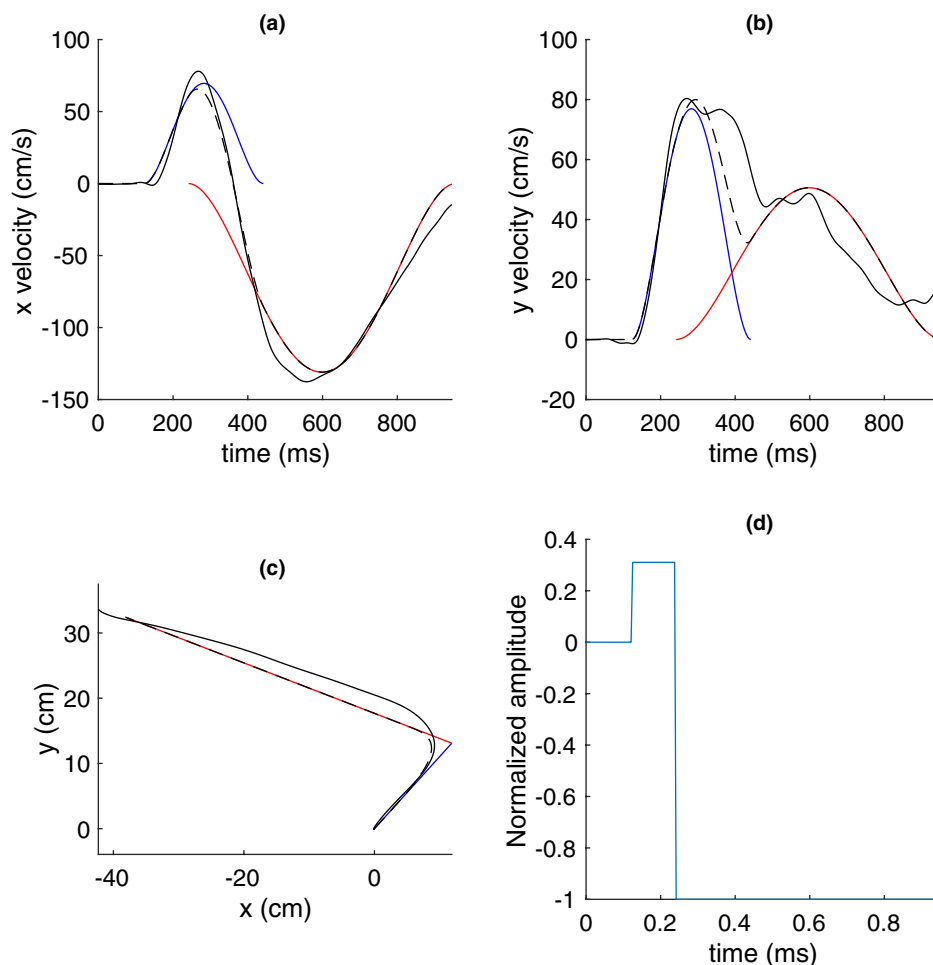


Fig. 4 An example of how the submovement decomposition is performed, and the cumulative submovement amplitude extracted on a trial-by-trial basis. The best-fit submovements, shown in blue and red, are found in terms of velocity, fit simultaneously for the **a** x velocity and **b** y velocity. The lines in black show the actual velocity. The dotted lines show the reconstructed trajectory from a summation of the submovements. **c** The reconstructed position. The origin, defined as the start point, was set on an individual basis based on a recording prior to the experiment **d** shows the normalized cumulative submove-

ment amplitude for this trial. The amplitude of the first submovement was 31% of the way to the right target, hence it has a normalized amplitude of 0.31. The amplitude of the second submovement is -131% , which takes it all the way to the left target. Hence, the second submovement has a normalized amplitude of -1.31 , and the cumulative submovement amplitude (CSA) at the end of the trial is -1 . All trials for a given condition/target direction are averaged, by participant, for the remainder of the analysis

Using the submovement decomposition, we were able to then compute the distance planned in the left–right direction (x) as a function of time. We use this direction and discard the front–back direction (y) as the component of the movement in this direction is not directly related to the decision process. We then analyze the movements for each participant, separately for each modality (visual and somatosensory), target direction (left and right), and congruence (congruent and incongruent). We normalize the amplitude of each submovement, such that a submovement that goes from the start position all the way to the right target will have an amplitude of $+1$, or -1 if it goes to the left target. For each of these eight conditions, we compute the cumulative submovement amplitude (CSA) by averaging the sum of the

normalized submovement amplitudes that begin before each time point, with negative values corresponding to movement to the left. Initially, the CSA will be zero (before any submovements have been made), and when all movements have been planned, the CSA will be 1 for movements to the right target, or -1 for movements to the left target. As we are interested in the CSA as a function of time after stimulus onset, no normalization for time or movement duration is performed. The CSA was assumed to be zero before movement onset. For the statistical analyses, we pooled the movements towards the left and right, after changing the sign of the movements towards the left such that positive values correspond to the direction of the correct target. Due to the normalization applied, CSA does not have units.

In our analysis, we assume that the CSA is analogous to the amount of accumulated information. This is based on the claim that when the participant begins a submovement, they will use the available information to plan their movement (Finkbeiner, & Friedman, 2011; Friedman et al., 2013), i.e., they will optimally use the information at hand to plan their movements (Trommershäuser, Maloney, & Landy, 2008). We note that the CSA technique means that each submovement only informs us about the decision process at the time of submovement onset. Thus, to sample the decision process at a range of times, we used three different SOAs to help ensure that submovements would be produced at a variety of times.

Fitting the activation–inhibition model

We fit a model that assumes there is an initial activation (A) of the irrelevant stimuli, followed by an inhibition (I), which we term the activation–inhibition (AI) model, based on the model described in Ridderinkhof (2002). We base our modeling on the assumption that the CSA is analogous to the amount of accumulated information. Further, we assume that the observed values for the congruent case consist of the sum of the accumulated information for the controlled process and for the congruent automatic process. Similarly, the incongruent case is the sum of the information accumulated for the controlled process and the incongruent automatic process. The two automatic processes are assumed to have equal magnitude but opposite sign; we discuss this limitation further in the discussion. Thus, if we sum the congruent and incongruent components, the automatic components will be canceled out, and we will be left with a quantity analogous to the controlled process. In a similar way, if we take the difference of the congruent and incongruent CSAs, we are left with the automatic component. For both these values, we take half the sum/difference to keep the same scale. In this way, the controlled and automatic processes were derived from the CSA for each participant, and then averaged across participants. We fit a straight line to the controlled process (two parameters: onset time and slope). For the automatic process, we fit straight lines for both the activation and the inhibition (four parameters: activation onset time and slope, inhibition onset time and slope). The parameters are found using a nonlinear programming solver (*fminsearch* function in Matlab). We compared the four parameters between modalities using the paired *t*-tests.

In addition to the modeling, we also directly compared the automatic process (also known as the congruence effect; Finkbeiner, & Friedman, 2011 or the Simon effect) between the two stimulus modalities, as well as the controlled process. We used a permutation procedure (Blair, & Karniski, 1993) to determine when the quantity was greater than 0 (Finkbeiner, & Friedman, 2011). We quantified the

asymmetry of the automatic process by fitting the automatic process for each participant to an ex-Gaussian (the sum of a Gaussian and exponential distribution), which has the parameters μ , σ and τ . The parameters μ and σ describe the Gaussian, while the τ parameter quantifies the size of the exponential “tail”—the larger the value of τ , the larger the tail and the greater the asymmetry. A perfect Gaussian distribution would have a τ of zero. We used the paired *t*-tests to compare the ex-Gaussian parameters between the modalities.

Results

Accuracy

The participants were able to perform the task, achieving relative high accuracy, which was defined as ending the movement at the correct target without touching the other targets (visual: median 99.7%, range 97.8–100%; somatosensory: median 95.5%, range 77.3–100%). In the visual task, the accuracy was greater than in the somatosensory task (Wilcoxon signed-rank test: $z = -3.48$, $p < 0.001$). For the remainder of the analysis, we only consider the correct trials.

Congruent and incongruent movements show different trajectories

As expected, the trajectories of the congruent and incongruent movements were different, as were the trajectories between modalities. The mean trajectories are shown in Fig. 5a. The bias towards initially making movements to the right can be clearly observed. Additionally, the incongruent trajectories take a less direct, longer path to get to the target. We note that the left and right targets are at slightly different distances from the start point, because we define the target location for each subject in a pre-experiment calibration based on the location of the sensor taped on the fingernail while the participant touches the wooden target. The difference is caused by differences in the relative position of the fingernail to the target when touching the left or right targets.

The *x* velocities of the movements were fit to orthogonal polynomials using the OPTA procedure, and then averaged across participants. Due to the range of onset times of the movement which resulted from the experimental protocol, we are able to look at the trajectories as a function of onset time. Each trajectory represents the movements that started at a particular time, with the bins ranging from approximately 50–400 ms post-stimulus, see Fig. 5b, with relatively little difference between the conditions. As can be observed in Fig. 5c, for the incongruent condition, the participants initially start heading towards the wrong (direct) target (shown

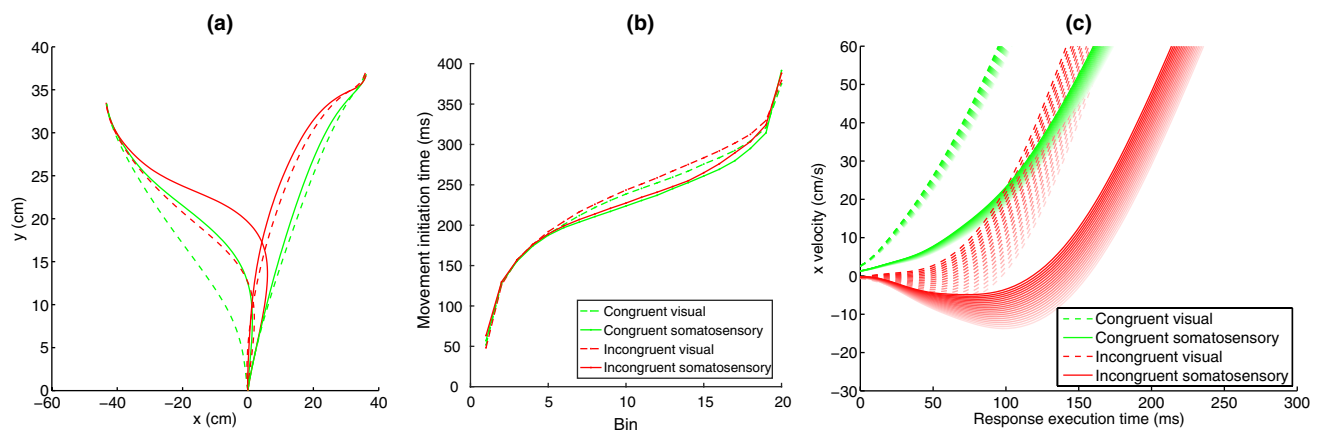


Fig. 5 **a** Mean trajectories for congruent and incongruent movements, averaged across all participants, for visual and somatosensory stimuli to the two targets. Note that as in most experiments with this response type, there is an initial bias to move towards the right. **b** Mean movement initiation time (MIT) bins used in the OPTA analysis, averaged across left and right movements and across participants. **c** Mean *x* velocities, averaged across left and right movements and across par-

ticipants, binned according to movement onset time, after the OPTA procedure. The darker the line, the later the onset time. Positive *x* velocities correspond to the direction of the correct target. Note that the movements are plotted relative to movement onset time (Fig. 5b), and not stimulus onset time, and there is the same number of bins (shown in Fig. 5b) for each condition

by the negative velocities), while this is not the case for the congruent trials. Further, the magnitude of this velocity in the wrong direction decreases as a function of movement onset time—the darker (later) trajectories head less in the wrong direction.

Comparison of results to the AI model

We compared the results of the study to the AI model by finding components of the CSA that are analogous to the controlled process and the automatic process. The mean values of these quantities, together with the CSA, are shown in Fig. 6a, b. We then fit a straight line to the controlled process, and activation and inhibition components to the automatic process. Good fits were achieved (correlation coefficient > 0.9) for both quantities for 16 of the 18 participants: 2 participants were not included in the subsequent analyses. The means and standard deviations of the fits can be found in Table 1, and these mean values were used to simulate the AI process (Fig. 6c, d). For both processes, we found that the automatic process started earlier than the controlled process [visual: automatic: 126 ± 9 ms, controlled: 163 ± 8 , $t(15) = -6.24$, $p < 0.001$; tactile: automatic: 120 ± 8 ms, controlled: 168 ± 9 ms, $t(15) = -5.84$, $p < 0.001$], although the onset times of both processes were not significantly different between the stimulus modalities. The slope of the controlled process was significantly higher for the visual stimuli, corresponding to a larger drift rate. Likewise, for the automatic process, the slope for both the automatic activation and inhibition was higher for the visual stimuli, i.e., the Simon effect had a shorter duration for the visual stimuli.

Time course of the Simon effect

Differences can be observed in the decision process between the visual and somatosensory stimuli, as was quantified above with the AI model. To allow a more fine-grained comparison, we use permutation analysis to determine when the automatic process (congruence/Simon effect) and the controlled process differ from zero, which is shown in Fig. 7.

Time course of the Simon effect

The automatic process (Fig. 7a) begins slightly earlier for the visual stimuli (104 ms) than the somatosensory stimuli (125 ms), but the effect of both ended at approximately the same time (650 ms). The lack of difference in end times may partially be a result of the significantly larger variation between participants for the somatosensory stimuli. However, there is a difference in the symmetry of the automatic process. While for the visual task, the automatic process is approximately symmetrical, for the somatosensory task, it has a much longer tail. This is confirmed by comparing the τ value from ex-Gaussians fit for each participant. For the somatosensory stimuli, τ was significantly larger (0.13 ± 0.02) than for the visual stimuli (0.08 ± 0.01), $t(17) = -3.1$, $p = 0.007$, although for both modalities, the τ value was significantly greater than 0 [visual: $t(17) = 6.3$, $p < 0.001$; somatosensory: $t(17) = 8.6$, $p < 0.001$].

We note that the time of the peak magnitude of the effect, the μ parameter, was also later for the somatosensory stimuli (254 ± 14 ms) compared to the visual stimuli (238 ± 14 ms), while the σ parameter was not significantly different between the modalities [visual: 0.057 ± 0.007 ; somatosensory: 0.065 ± 0.009 , $t(17) = -0.74$, $p = 0.47$]. The controlled process (Fig. 7b) starts earlier for the visual (121 ms) compared to the somatosensory stimuli (133 ms), as defined by the

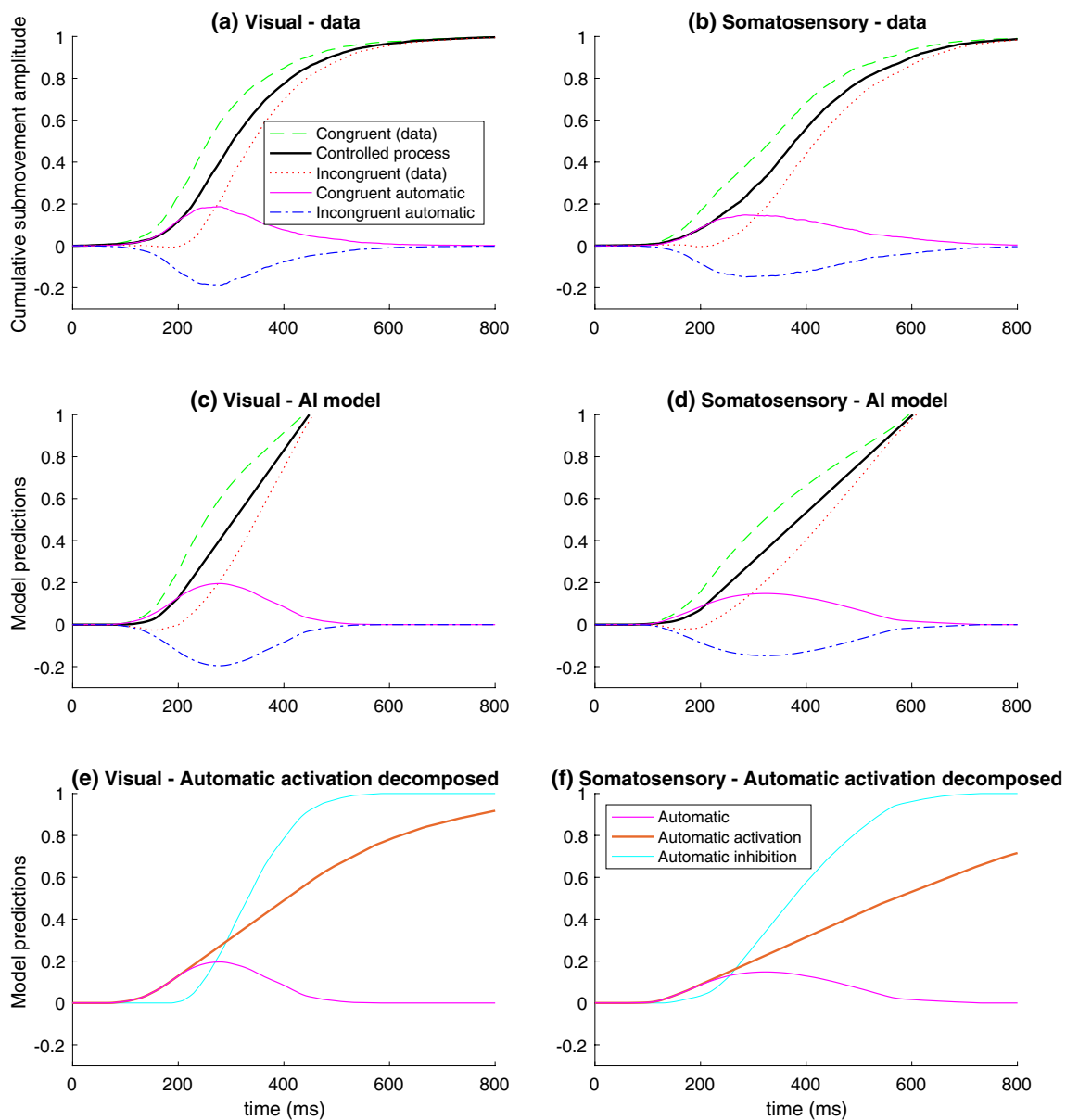


Fig. 6 Mean cumulative submovement amplitudes and AI model predictions. Cumulative submovement amplitudes for the **a** visual and **b** somatosensory trials, averaged across participants. The green and red lines correspond to the mean cumulative submovement amplitudes in the congruent and incongruent cases, respectively. The purple and blue lines represent the congruent and incongruent automatic compo-

nents, respectively. The black line is the controlled process. **c, d** The mean behavior of the AI model with the best-fit parameters to the CSA data. **e, f** The decomposition of the automatic activation (i.e., the purple line from **c** to **d**) into the activation (A) and inhibition (I) components. For both models, the best-fit data were found for each subject (see Table 1); the graphs show the average across subjects

Discussion

In this study, we compared the time course of the Simon effect for visual and somatosensory stimuli using arm movements. Based on the cumulative submovement

amplitudes, we were able to recover the controlled and automatic processes used by the participants, which showed a strong similarity to the activation/inhibition patterns predicted by the activation–inhibition (AI) model. Using this analysis, we confirmed the previously reported quantitative differences in the Simon effect for visual and somatosensory stimuli. We found that a single model was able to describe both the visual and somatosensory Simon tasks. The differences in parameter fits are consistent with an activation of the automatic process that is inhibited at

Table 1 Model parameters fit to the controlled and automatic processes, calculated from the cumulative submovement amplitudes

Parameters	Visual	Somatosensory	$t(15)$	p value
Controlled process				
Onset time (ms)	163 ± 8	168 ± 9	- 0.78	0.45
Slope (s ⁻¹)	3.52 ± 0.18	2.31 ± 0.08	8.14	< 0.001
Automatic process				
Activation onset time (ms)	126 ± 9	120 ± 8	0.72	0.48
Activation slope (s ⁻¹)	1.80 ± 0.16	1.13 ± 0.13	4.02	0.001
Inhibition onset time (ms)	117 ± 7	100 ± 13	0.97	0.35
Inhibition slope (s ⁻¹)	5.74 ± 0.42	3.38 ± 0.28	5.36	< 0.001

The parameters were fit for each participant, and the values shown are the mean ± standard error across the 16 participants where successful fits could be made for both stimuli. The last two columns are the result of comparisons between the parameters fit to the visual and somatosensory stimuli using paired t -tests (t score and p value)

a significantly slower rate for the somatosensory stimuli compared to the visual stimuli.

The results presented here are consistent with the time difference rather than magnitude difference account of the Simon effect (Finkbeiner, & Heathcote, 2016; Proctor et al., 2011). We found that the automatic process starts significantly earlier than the controlled process. The automatic process reaches its peak relatively early (after approximately

250 ms) and then decays, whereas the controlled process accumulates evidence in an approximately linear fashion, as would be expected by a diffusion process. Further evidence of the temporal differences between the automatic and controlled processes was shown by the initial velocity of incongruent movements that headed in the direction of the stimuli location (Finkbeiner, & Heathcote, 2016). This is also similar to the partial errors observed early in EMG recordings (Servant et al., 2016).

A primary finding of this study was that the somatosensory stimuli showed lower values for the slopes for all three processes (controlled activation, automatic activation and inhibition) compared to the visual stimuli, but not for onset times of these processes, as was predicted. In contrast, analysis of the time course of the Simon effect did find small differences in the onset times, although this technique does not provide a way to test whether this difference is statistically significant. We assumed that as both stimuli are clearly distinguishable, they would have similar rates of uptake [i.e., mean slope, similar to the drift rate in diffusion models (Ratcliff, 2006)], although the differences in slopes observed did not support this hypothesis. In earlier studies (Salzer, 2013; Salzer et al., 2014), we demonstrated that the average response time in the visual Simon task was 100–180 ms faster than in the somatosensory Simon task. This finding led us to assume that the processing of the somatosensory information would be slower. Different onset times would

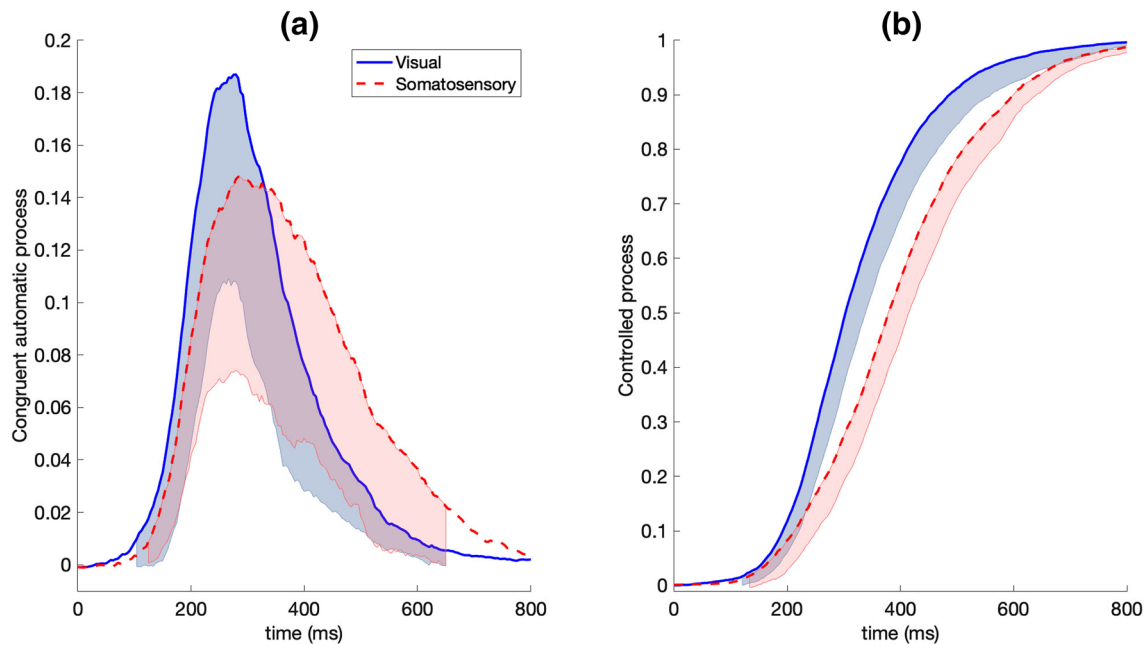


Fig. 7 a Automatic process (congruence/Simon effect): the CSA for the congruent stimuli minus the CSA for the incongruent stimuli, pooled for left and right movements. The shaded area is the 95% confidence intervals, it is shown only when the lower bound of the confidence interval is greater than zero. The congruence effect begins

slightly earlier for the visual stimuli and ends at approximately the same time, but it should be noted that there is much more variance between participants for the somatosensory task. **b** Controlled process: the sum of the CSA for the congruent and incongruent stimuli

have suggested differences in initial processing times of the stimuli (i.e., before it contributes to the decision-making process), however, this was not observed. The lack of difference is likely due to the similarity in the time at which somatosensory and visual information are first available to the cortex, as has been shown in previous studies. For example, Pruszynski et al. (2016) have found that corrections following perturbation onset took approximately 110 ms in either modality, which is similar to the times we found for the start of the automatic responses. In another study, it was found that the internal sensorimotor processing times before performing fast saccades were similar for visual (~ 140 ms) and for proprioceptive feedback (~ 126 to 136 ms) (Crevecoeur, Barrea, Libouton, Thonnard, & Lefèvre, 2017). Rather, the observed differences in the slopes—lower slopes for the somatosensory stimuli, suggest that there is a slower uptake of somatosensory information compared to visual information as a source for decision making, for both the controlled and automatic processes, but not slower initial access. The reason for this difference is an area that requires further investigation, although we note that it is in general problematic to match the salience and difficulty levels for stimuli from different modalities.

In contrast to comparisons of congruent and incongruent reaction time distributions (congruency effects), which can show hard-to-explain differences due to modality, direction, and external cues (Salzer, 2013), this technique allows a disassociation of the different contributions to processing time. We note that a recent study showed that the duration of the stimuli does not affect the time course of the automatic response (Ellinghaus, Karlbauer, Bausenhart, & Ulrich, 2018), whereas in this study we showed that the modality does have clear effects on the time course of the automatic response.

There is a debate in the literature regarding the effect of the stimuli location, as to whether the spatial aspect spontaneously decays with time (Hommel, 2009), or is actively suppressed (Ridderinkhof, 2002; van den Wildenberg, Wylie, Forstmann, Burle, Hasbroucq, & Ridderinkhof, 2010). While the analysis presented here is not able to differentiate between the two possibilities, it does provide constraints on the nature of the automatic process, in that the time course of the congruence effect is derived from the data and is observed in multiple modalities. In this study, the extraction of the automatic and controlled processes is essentially “model-free”, in that we did not need to assume anything about their time course or shape. In particular, the change in modality caused a difference in the shape of the activation of the automatic process. While a difference in the width of the Gaussian would speak in favor of spontaneous decay, a difference in the exponential parameter would suggest a difference in active suppression. While the σ (width) parameter was not different between the modalities, the

exponential parameter of the automatic process τ is larger for the somatosensory stimuli, i.e., the decay takes much longer than the increase to the peak effect. These differences between modalities were also observed in the different fits to a gamma function. The slower decay for the somatosensory stimuli is compatible with the notion of weaker selective suppression of the automatic process proposed by Ridderinkhof (2002).

While this study did not perform computational modeling of the trajectories, we note that the patterns that emerged from the submovement analysis are consistent with a gradual accumulation of evidence (Friedman et al., 2013), as submovements made prior to a final decision only go part of the way towards the target. Recent computational models, based on the drift diffusion model or similar processes have shown significant success in modeling multiple observable aspects (Ulrich et al., 2015; van Maanen, Turner, & Forstmann, 2015). The technique used in this study provides a more direct way of observing the automatic processes than is possible when only using response times.

Although arm movements allow us to obtain more than a single data point to fit per trial, and the ability to access the decision state before a final decision is made, there are also limitations to this approach. In particular, using arm movements necessarily changes the strategy used by the participants. For example, once a movement has been initiated in a certain direction, there exists a cost involved in changing direction (Marcos et al., 2015; Moher, & Song, 2014). Also, the total duration of the movements is longer than the typical reaction times observed, which may also affect the decision process (Wispiński, Gallivan, & Chapman, 2019). Additionally, the analysis performed was based on the assumption that difference between the controlled and observed processes in the two directions (i.e., congruent and incongruent) is equal in magnitude but have opposite signs, which may not always be the case (Aisenberg, & Henik, 2012). For the somatosensory Simon task, it is problematic to achieve a neutral condition, due to problems with placing the tactors on the middle of the back, i.e., on the spine (Salzer et al., 2014). We also note that our model assumed that the automatic activation and suppression are both linear processes, which may not be the case (Usher, & McClelland, 2001). This limitation likely led to the finding that the inhibition started before the automatic activation, which should not be possible (see Table 1). Determination of the time course of the inhibition process should be possible in the future by comparing the suitability of different, nonlinear models, or perhaps using process models (such as the drift diffusion model) for parts of the process. Further, it is possible that rather than active inhibition occurring, the process simply decays with time—additional modeling work may help in distinguishing between these two possibilities.

In conclusion, in this study, we examined the differences between the visual and somatosensory versions of the Simon task. By examining the intent of the participants, as measured using cumulative submovement amplitude, we were able to extract processes analogous to the controlled and automatic processes described in the activation–inhibition model. We found that the same relatively simple model was able to accurately explain the movements performed for both visual and somatosensory Simon effects. The differences between the modalities were observed not in the onset of activation, but rather the rate of activation and inhibition, i.e., these differences were mostly quantitative rather than qualitative. The novel technique described here has the potential to help deepen our understanding of the processes involved in resolving conflict during decision making.

Acknowledgements We thank Maayan Ben Nun for performing the data collection.

Data availability The datasets used during the current study are available from the corresponding author on reasonable request.

Funding This research did not receive any specific grant from funding agencies in the public, commercial, or not-for-profit sectors.

Compliance with ethical standards

Conflict of interest The authors declare that they have no conflict of interest.

References

- Aisenberg, D., & Henik, A. (2012). Stop being neutral: Simon takes control! *Quarterly Journal of Experimental Psychology*, *65*(2), 295–304. <https://doi.org/10.1080/17470218.2010.507819>.
- Blair, R. C., & Karniski, W. (1993). An alternative method for significance testing of waveform difference potentials. *Psychophysiology*, *30*(5), 518–524. <https://doi.org/10.1111/j.1469-8986.1993.tb02075.x>.
- Brainard, D. H. (1997). The psychophysics toolbox. *Spatial Vision*, *10*(4), 433–436. <https://doi.org/10.1163/156856897X00357>.
- Buetti, S., & Kerzel, D. (2009). Conflicts during response selection affect response programming: Reactions toward the source of stimulation. *Journal of Experimental Psychology Human Perception and Performance*, *35*(3), 816–834. <https://doi.org/10.1037/a0011092>.
- Crevecoeur, F., Barrea, A., Libouton, X., Thonnard, J.-L., & Lefèvre, P. (2017). Multisensory components of rapid motor responses to fingertip loading. *Journal of Neurophysiology*, *118*(1), 331–343. <https://doi.org/10.1152/jn.00091.2017>.
- De Jong, R., Liang, C.-C., & Lauber, E. (1994). Conditional and unconditional automaticity: A dual-process model of effects of spatial stimulus–response correspondence. *Journal of Experimental Psychology Human Perception and Performance*, *20*(4), 731–750. <https://doi.org/10.1037/0096-1523.20.4.731>.
- Ellinghaus, R., Karlbauer, M., Bausenhart, K. M., & Ulrich, R. (2018). On the time-course of automatic response activation in the Simon task. *Psychological Research*, *82*(4), 734–743. <https://doi.org/10.1007/s00426-017-0860-z>.
- Finkbeiner, M., Coltheart, M., & Coltheart, V. (2014). Pointing the way to new constraints on the dynamical claims of computational models. *Journal of Experimental Psychology Human Perception and Performance*, *40*(1), 172–185. <https://doi.org/10.1037/a0033169>.
- Finkbeiner, M., & Friedman, J. (2011). The flexibility of nonconsciously deployed cognitive processes: Evidence from masked congruence priming. *PLoS One*, *6*(2), e17095. <https://doi.org/10.1371/journal.pone.0017095>.
- Finkbeiner, M., & Heathcote, A. (2016). Distinguishing the time- and magnitude-difference accounts of the Simon effect: Evidence from the reach-to-touch paradigm. *Attention Perception and Psychophysics*, *78*, 848–867. <https://doi.org/10.3758/s13414-015-1044-9>.
- Flash, T., & Henis, E. A. (1991). Arm trajectory modification during reaching towards visual targets. *Journal of Cognitive Neuroscience*, *3*(3), 220–230. <https://doi.org/10.1162/jocn.1991.3.3.220>.
- Flash, T., & Hogan, N. (1985). The coordination of arm movements: An experimentally confirmed mathematical model. *Journal of Neuroscience*, *5*(7), 1688–1703.
- Friedman, J. (2014). Repeated measures (computer software). <https://doi.org/10.5281/zenodo.10438>.
- Friedman, J., Brown, S., & Finkbeiner, M. (2013). Linking cognitive and reaching trajectories via intermittent movement control. *Journal of Mathematical Psychology*, *57*(3–4), 140–151. <https://doi.org/10.1016/j.jmp.2013.06.005>.
- Friedman, J., & Finkbeiner, M. (2010). Temporal dynamics of masked congruence priming: Evidence from reaching trajectories. In W. Christensen, E. Schier, & J. Sutton (Eds.), *Proceedings of the 9th conference of the Australasian Society for Cognitive Science* (pp. 98–105). Sydney: Macquarie University. <https://doi.org/10.5096/ascs200916>.
- Hommel, B. (1994). Spontaneous decay of response-code activation. *Psychological Research*, *56*(4), 261–268. <https://doi.org/10.1007/BF00419656>.
- Hommel, B. (2009). Action control according to TEC (theory of event coding). *Psychological Research*, *73*(4), 512–526. <https://doi.org/10.1007/s00426-009-0234-2>.
- Horowitz, J., Majeed, Y. A., & Patton, J. (2016). A fresh perspective on dissecting action into discrete submovements. In *2016 38th annual international conference of the IEEE Engineering in Medicine and Biology Society (EMBC)* (pp. 5684–5688). Presented at the 2016 38th Annual International Conference of the IEEE Engineering in Medicine and Biology Society (EMBC). <https://doi.org/10.1109/embc.2016.7592017>.
- Karayanidis, F., Provost, A., Brown, S., Paton, B., & Heathcote, A. (2011). Switch-specific and general preparation map onto different ERP components in a task-switching paradigm. *Psychophysiology*, *48*(4), 559–568. <https://doi.org/10.1111/j.1469-8986.2010.01115.x>.
- Marcos, E., Cos, I., Girard, B., & Verschure, P. F. M. J. (2015). Motor cost influences perceptual decisions. *PLoS One*, *10*(12), e0144841. <https://doi.org/10.1371/journal.pone.0144841>.
- Moher, J., & Song, J.-H. (2014). Perceptual decision processes flexibly adapt to avoid change-of-mind motor costs. *Journal of Vision*, *14*(8), 1–13. <https://doi.org/10.1167/14.8.1>.
- Proctor, R. W., Miles, J. D., & Baroni, G. (2011). Reaction time distribution analysis of spatial correspondence effects. *Psychonomic Bulletin and Review*, *18*(2), 242–266. <https://doi.org/10.3758/s13423-011-0053-5>.
- Pruszynski, J. A., Johansson, R. S., & Flanagan, J. R. (2016). A rapid tactile-motor reflex automatically guides reaching toward handheld objects. *Current Biology*, *26*(6), 788–792. <https://doi.org/10.1016/j.cub.2016.01.027>.
- Ratcliff, R. (1979). Group reaction time distributions and an analysis of distribution statistics. *Psychological Bulletin*, *86*(3), 446–461.
- Ratcliff, R. (2006). Modeling response signal and response time data. *Cognitive Psychology*, *53*(3), 195–237. <https://doi.org/10.1016/j.cogpsych.2005.10.002>.

- Ratcliff, R., & McKoon, G. (2008). The diffusion decision model: Theory and data for two-choice decision tasks. *Neural Computation*, 20(4), 873–922. <https://doi.org/10.1162/neco.2008.12-06-420>.
- Ridderinkhof, K. R. (2002). Activation and suppression in conflict tasks: empirical clarification through distributional analyses. In W. Prinz & B. Hommel (Eds.), *Common mechanisms in perception and action* (pp. 494–519). Oxford: Oxford University Press.
- Rohrer, B., & Hogan, N. (2006). Avoiding spurious submovement decompositions II: A scattershot algorithm. *Biological Cybernetics*, 94(5), 409–414. <https://doi.org/10.1007/s00422-006-0055-y>.
- Salzer, Y. (2013). *Cognitive control in the tactile Simon task: The unique role of tactile spatial information (PhD)*. Beer-Sheva: Ben-Gurion University of the Negev.
- Salzer, Y., Aisenberg, D., Oron-Gilad, T., & Henik, A. (2014). In touch with the Simon effect. *Experimental Psychology*, 61(3), 165–179. <https://doi.org/10.1027/1618-3169/a000236>.
- Salzer, Y., de Hollander, G., & Forstmann, B. U. (2017). Sensory neural pathways revisited to unravel the temporal dynamics of the Simon effect: A model-based cognitive neuroscience approach. *Neuroscience & Biobehavioral Reviews*. <https://doi.org/10.1016/j.neubiorev.2017.02.023>.
- Schwarz, W., & Miller, J. (2012). Response time models of delta plots with negative-going slopes. *Psychonomic Bulletin and Review*, 19(4), 555–574. <https://doi.org/10.3758/s13423-012-0254-6>.
- Scorolli, C., Pellicano, A., Nicoletti, R., Rubichi, S., & Castiello, U. (2014). The Simon effect in action: Planning and/or on-line control effects? *Cognitive Science*, 39(5), 972–991. <https://doi.org/10.1111/cogs.12188>.
- Servant, M., White, C., Montagnini, A., & Burle, B. (2016). Linking theoretical decision-making mechanisms in the Simon task with electrophysiological data: A model-based neuroscience study in humans. *Journal of Cognitive Neuroscience*, 28(10), 1501–1521. https://doi.org/10.1162/jocn_a_00989.
- Simon, J. R. (1990). The effects of an irrelevant directional cue on human information processing. In R. W. Proctor & T. G. Reeve (Eds.), *Advances in psychology* (Vol. 65, pp. 31–86). North-Holland. [https://doi.org/10.1016/s0166-4115\(08\)61218-2](https://doi.org/10.1016/s0166-4115(08)61218-2).
- Simon, J. R., & Wolf, J. D. (1963). Choice reaction time as a function of angular stimulus–response correspondence and age. *Ergonomics*, 6(1), 99–105. <https://doi.org/10.1080/00140136308930679>.
- Spivey, M. J., Grosjean, M., & Knoblich, G. (2005). Continuous attraction toward phonological competitors. *Proceedings of the National Academy of Sciences of the United States of America*, 102(29), 10393–10398. <https://doi.org/10.1073/pnas.0503903102>.
- Töbel, L., Hübner, R., & Stürmer, B. (2014). Suppression of irrelevant activation in the horizontal and vertical Simon task differs quantitatively not qualitatively. *Acta Psychologica*, 152, 47–55. <https://doi.org/10.1016/j.actpsy.2014.07.007>.
- Trommershäuser, J., Maloney, L. T., & Landy, M. S. (2008). Decision making, movement planning and statistical decision theory. *Trends in Cognitive Sciences*, 12(8), 291–297. <https://doi.org/10.1016/j.tics.2008.04.010>.
- Ulrich, R., Schröter, H., Leuthold, H., & Birngruber, T. (2015). Automatic and controlled stimulus processing in conflict tasks: Superimposed diffusion processes and delta functions. *Cognitive Psychology*, 78, 148–174. <https://doi.org/10.1016/j.cogpsych.2015.02.005>.
- Usher, M., & McClelland, J. L. (2001). The time course of perceptual choice: The leaky, competing accumulator model. *Psychological Review*, 108(3), 550–592. <https://doi.org/10.1037/0033-295X.108.3.550>.
- van den Wildenberg, W. P. M., Wylie, S. A., Forstmann, B. U., Burle, B., Hasbroucq, T., & Ridderinkhof, K. R. (2010). To head or to heed? Beyond the surface of selective action inhibition: A review. *Frontiers in Human Neuroscience*, 4, 222. <https://doi.org/10.3389/fnhum.2010.00222>.
- van Maanen, L., Turner, B., & Forstmann, B. U. (2015). From model-based perceptual decision-making to spatial interference control. *Current Opinion in Behavioral Sciences*, 1, 72–77. <https://doi.org/10.1016/j.cobeha.2014.10.010>.
- Wascher, E., Schatz, U., Kuder, T., & Verleger, R. (2001). Validity and boundary conditions of automatic response activation in the Simon task. *Journal of Experimental Psychology Human Perception and Performance*, 27(3), 731–751. <https://doi.org/10.1037/0096-1523.27.3.731>.
- Welsh, T. N., Pacione, S. M., Neyedli, H. F., Ray, M., & Ou, J. (2015). Trajectory deviations in spatial compatibility tasks with peripheral and central stimuli. *Psychological Research*, 79(4), 650–657. <https://doi.org/10.1007/s00426-014-0597-x>.
- White, C. N., Servant, M., & Logan, G. D. (2018). Testing the validity of conflict drift-diffusion models for use in estimating cognitive processes: A parameter-recovery study. *Psychonomic Bulletin and Review*, 25(1), 286–301. <https://doi.org/10.3758/s13423-017-1271-2>.
- Wiegand, K., & Wascher, E. (2005). Dynamic aspects of stimulus–response correspondence: Evidence for two mechanisms involved in the Simon effect. *Journal of Experimental Psychology Human Perception and Performance*, 31(3), 453–464. <https://doi.org/10.1037/0096-1523.31.3.453>.
- Wiegand, K., & Wascher, E. (2007). The Simon effect for vertical S–R relations: Changing the mechanism by randomly varying the S–R mapping rule? *Psychological Research*, 71(2), 219–233. <https://doi.org/10.1007/s00426-005-0023-5>.
- Wispirski, N. J., Gallivan, J. P., & Chapman, C. S. (2019). Models, movements, and minds: Bridging the gap between decision making and action. *Annals of the New York Academy of Sciences*. <https://doi.org/10.1111/nyas.13973>.
- Woestenburg, J. C., Verbaten, M. N., van Hees, H. H., & Slangen, J. L. (1983). Single trial ERP estimation in the frequency domain using orthogonal polynomial trend analysis (OPTA): Estimation of individual habituation. *Biological Psychology*, 17(2–3), 173–191. [https://doi.org/10.1016/0301-0511\(83\)90018-2](https://doi.org/10.1016/0301-0511(83)90018-2).
- Xiong, A., & Proctor, R. W. (2016). Decreasing auditory Simon effects across reaction time distributions. *Journal of Experimental Psychology Human Perception and Performance*, 42(1), 23–38. <https://doi.org/10.1037/xhp0000117>.

Publisher's Note Springer Nature remains neutral with regard to jurisdictional claims in published maps and institutional affiliations.